筑　波　大　学

博 士 （医 学） 学 位 論 文

p62 modulates the intrinsic signaling of UVB-induced apoptosis

（p62 は UVB 刺激によるアポトーシスの
内因性シグナル伝達を調節する）

２０１６

筑波大学大学院博士課程人間総合科学研究科
伊藤　佐知子

Contents

Title

p62 modulates the intrinsic signaling of UVB-induced apoptosis

Running Title

p62 modulates UVB-induced apoptosis

Authors

Sachiko Ito

Abbreviations

ROS, reactive oxygen species; UV, ultraviolet; PCR, polymerase chain reaction; MEF, mouse embryo fibroblast; RIPA buffer, radioimmunoprecipitation assay buffer; PVDF, polyvinylidene difluoride; PI, propidium iodide; Bcl-2, B-cell lymphoma 2; Bcl-xL, B-cell lymphoma-extra large; Bax, Bcl-2–associated X protein; PUMA, p53 upregulated modulator of apoptosis; Noxa, Phorbol-12-myristate-13-acetate-induced protein 1; ATM, Ataxia telangiectasia mutated; ATR, ATM- and RAD3-related; Stat3, signal transducer and activator of transcription 3; SRC, SRC proto-oncogene; PIKK, phosphatidylinositol 3-kinase-related kinases; UVRAG, UV radiation resistance-associated gene protein; Beclin1, Bcl-2 interacting protein 1.

ABSTRACT

Background: UVB radiation is the main source of sunburn and skin cancers. Apoptosis eliminates photodamaged cells, and is thus important for preventing epidermal carcinogenesis. The cytoplasmic regulatory protein p62/A170/sequestosome 1 (p62) molecule is involved in a variety of cellular and signaling pathways. p62 is known to be important in autophagy, but its role in UVB-induced apoptosis remains to be clarified.

Objective: To investigate the role of p62 against UVB-induced apoptotic changes, using mouse embryonic fibroblasts (MEFs) derived from p62 homozygous knockout ($p62^{-/-}$) mice.

Methods: $p62^{-/-}$ and wild-type ($p62^{+/+}$) MEFs were subjected to UVB irradiation, and the resultant apoptosis was analyzed using flow cytometry, quantitative real-time PCR, and western blots.

Results: Apoptosis was decreased in the $p62^{-/-}$ MEFs compared to $p62^{+/+}$ MEFs in response to UVB treatment. Compared with $p62^{+/+}$ MEFs, $p62^{-/-}$ MEFs expressed significantly more Bcl-2 and less Bax, and showed increased Src and Stat3 phosphorylation. Our results show that p62 regulates apoptotic pathways by modifying critical signaling intermediates such as Src and Stat3.

Conclusion: p62 deficiency reduces UVB-induced apoptosis by modulating intrinsic apoptotic signaling through Src phosphorylation.

Keywords: p62, UVB, apoptosis, ROS

1. Introduction

Ultraviolet B (UVB) radiation is one of the most important stimuli affecting the epidermis. UVB (280-315nm) enters the dermis, which is only partially blocked by clouds or fog. UVB radiation can cause skin redness and is considered the main cause of sunburn and skin cancers. Induction of DNA damage by UVB may generate mutations and genomic instability leading to carcinogenesis [1]. However epidermal cells that are irreparably damaged by excessive UVB exposure are cleared by apoptosis to avoid malignant transformation. DNA repair mechanisms, the damaged skin cells can be eliminated by induction of apoptosis, which is mediated through the action of tumor suppressor. Therefore, suppression of the apoptosis machinery is thought to lower the threshold for the occurrence of a cancer. Thus, apoptosis is important in preventing skin cancers [2, 3].

UVB-induced apoptosis is a complex event that involves several pathways, including the extrinsic and intrinsic apoptosis signaling pathways. The extrinsic pathway acts through the fibroblast-associated tumor necrosis factor (TNF) receptor and other death receptors, which activate a caspase cascade in response to ligand binding. The intrinsic apoptosis pathway is regulated by the Bcl-2 family of proteins, which includes both anti-apoptotic (Bcl-2, Bcl-xl, Bcl-w) and pro-apoptotic (Bax, Bak, Bid) members. Balance between anti-apoptotic and pro-apoptotic proteins determines whether apoptosis is induced or prevented [2]. These Bcl-2 proteins are crucial regulators of epidermal homeostasis and cell fate in stressed skin, and are involved in skin carcinogenesis and responses to cancer therapy [4].

The cytoplasmic protein p62/A170/sequestosome 1 is a multifunctional signaling molecule that is involved in a variety of cellular pathways [5]. Murine p62, formerly called A170, was cloned as an oxidative-stress-inducible protein by Ishii's group [6]. p62 regulates autophagy by interacting directly with LC3 [7]; it also interacts with other key components of various signaling mechanisms, and is required for tumor transformation [8, 9]. p62 has important roles in cell growth and cancer, through its functions as a regulator of autophagy, as a key factor in nutrient sensing and in genomic stability, and as an inducer of oxidative detoxifying proteins [5]. Many studies report crosstalk between autophagy and apoptosis [10], and p62 is associated with both of these functions. p62 is also implicated in activating the transcription factor NF-κB and in restraining ROS production and inhibiting tumor-cell death [8, 9]. The overexpression of p62 has been found in various cancers such as lung carcinoma and hepatocellular carcinoma in recent years, so it is recognized to be involved in the cancer development. It has been found that suppression of NF-κB signal due to deletion of p62 gene suppresses ras-induced lung adenocarcinoma formation, that increased expression of p62 due to constitutive K-ras activation is involved in development of pancreatic duct adenocarcinoma, and that abnormally elevated NF-κB signal via p62 accumulation in autophagy-deficient tumor cells might partially promote carcinogenesis [5,11]. In addition, it has been reported that expression of p62 in SCC and cutaneous melanoma is enhanced in skin cancer. In SCC, the positive rate of p62 decreases as the stage progresses, whereas in melanoma it does not correlate with stage progression, and the role of p62 in skin cancer remains unclear [12,13]. As above stated, many researchers maintain that p62 promotes the carcinogenesis.

However a previous study suggested that p62-deficient cells are highly proliferative,

and that p62 inhibits proliferation [14]. In this study, we sought to clarify the role of p62 in UVB-induced apoptosis by focusing on the intrinsic apoptotic signaling pathway (Fig.1).

2. Materials and methods

2.1. Cell culture

Gene-recombination experiments were authorized by the University of Tsukuba Gene Recombination Experiment Safety Committee (authorization No. 14-369). We obtained $p62^{-/-}$ and $p62^{+/+}$ mouse embryonic fibroblasts (MEFs) as previously described [15]. Briefly, the brain and dark-red (internal) organs were dissected away from the embryos, the remaining tissue was finely minced, and the cells were dissociated using 0.25% trypsin, which was removed by centrifugation. The resulting MEFs and human keratinocytes of the HaCaT cell line were cultured in Dulbecco's modified Eagle's medium (DMEM) containing streptomycin (100 U/ml), penicillin (0.1 mg/ml), and heat-inactivated 10% FBS. The cells were cultured in a humidified atmosphere with 5% CO_2 at 37 °C. All of the measurements in experiments with MEF subcultures derived from different stock and HaCaT cell line were obtained from three individual culture plates (n=3).

2.2. Knockdown experiments

All of the siRNA experiments used Stealth™ RNAi (Thermo Fisher Scientific, Yokohama, Japan). The primers AAUGUGUCCAGUCAUCGUCUCCUCC (sense) and GGAGGAGACGAUGACUGGACACAUU (antisense) were used for mouse p62 siRNA (Qiagen, Venlo, Netherlands), and Stealth-RNAi negative universal control was used for a negative control. For transfection, 3 μl of lipofectamine RNAiMAX (Thermo Fisher) and 3 μl of siRNAwere added to 500 μl of opti-MEM, and the mixture was incubated for

15 min at room temperature, added to cell cultures, and incubated for 24 h at 37 °C in a CO_2 incubator.

2.3. UV irradiation

For irradiation, the culture medium was replaced by an irradiation culture medium with 30 mM HEPES pH 7.4 and without phenol red, and the cells were UV-irradiated by an FL20SE UV lamp (Toshiba, Tokyo, Japan). The dose of UVB irradiation was measured using a radiometer (UVR-305 / 365; Toshiba, Tokyo, Japan). After UV irradiation, the medium was replaced by regular culture medium, and the cells were incubated at 37 °C.

2.4. Analysis of apoptosis using flow cytometry

UVB-induced apoptosis was assessed with an Annexin V-FLUOS Staining Kit (Roche Diagnostic. Co., Tokyo) followed by flow cytometry. Cells were seeded at 1×10^5 cells per 35-mm dish, cultured overnight in DMEM containing 10% FBS, and then irradiated with UVB. After 5 h the cells were washed, resuspended, and stained with fluorescein isothiocyanate (FITC)-conjugated Annexin V antibody and propidium iodide (PI) according to the manufacturer's instructions. The cells (2×10^4 per sample) were then analyzed using a flow cytometer (FACSCalibur; Becton Dickinson Co., Tokyo) equipped with a 488-nm argon laser and CellQuest Pro software. The apoptosis ratio was defined as the percentage of cells in the upper- and lower-right quadrants (late and early apoptosis: PI-positive area), and was measured as previously reported [16] [17, 18].

2.5. Western blots

Whole-cell extracts were generated by lysing cells in RIPA buffer (50 mM Tris-HCl pH 7.4, 150 mM EDTA, 1% TritonX 100, 1% sodium deoxycholate, and 0.1% SDS) 24h after UVB irradiation, followed by centrifugation and collection of the supernatants. The samples were separated on an SDS polyacrylamide gel by electrophoresis and then transferred onto PVDF membranes for 2 h at 80 V. The membranes were incubated with the primary antibody (diluted 1:1000) for 1 h at room temperature. Anti-Bcl-2 (#2876), anti-Bcl-xL (#2762), anti-Bax (#2772), anti-phospho Src (#2101), anti-Src (#2108), anti-phospho Stat3 (#5185), and anti-Stat3 (#9132) antibodies were purchased from Cell Signaling Technology (Tokyo, Japan). Anti-actin antibody (A2103) was purchased from Sigma-Aldrich (Tokyo, Japan). 4-amino-5-(4-chlorophenyl)-7-(dimethylethyl) pyrazolo [3,4-d]pyrimidine (PP2) (Wako Pure Chemical Industries Ltd. Tokyo, Japan), a inhibitor of src-family kinases was treated 12h before UVB irradiation. After treatment with peroxidase-conjugated anti-mouse IgG antibody (Sigma-Aldrich) or anti-rabbit IgG antibody (Jackson ImmunoResearch, West Grove, USA) for 1 h at room temperature, the labeled bands were detected with the ECL Plus Kit (GE Healthcare Bio-Sciences Co., Tokyo, Japan). The band density was quantified by using image analysis software (Image J 1.46: National Institute of Mental Health, Bethesda, USA.).

2.6. Quantitative real-time PCR analysis

Quantitative real-time PCR was conducted as described previously [19, 20] using an ABI Prism 7000 (Thermo Fisher Scientific), and the mRNA expression levels were normalized to GAPDH, 20]. RNA was extracted from the cells using Sepasol (Nacalai, Tokyo, Japan) and subjected to electrophoresis at 100 V for 30 min. The following

primers were used: Bcl-2, forward ATGCCTTTGTGGAACTATATGGC and reverse GGTATGCACCCAGAGTGATGC; Bcl-xL, forward CAGGTGCGTGGAAAGCGTA and reverse CCTGGGTAAGGGGAGGAGT; Bax, forward AGACAGGGGCCTTTTTGCTAC and reverse AATTCGCCGGAGACACTCG; PUMA, forward AGCAGCACTTAGAGTCGCC and reverse CCGCT CGTACTGTGCG TTGAG; NOXA, forwardGCAGAGCTACCACCTGAGTTC and reverse CTTTTGCGACTTCCCAGGCA; ATM, forward GATGGCTCATTTGGGCCG and reverse GTGTGGCTGATACATTTGA; and Survivin, forward ATCCACTGCCCTACCGAGAA and reverse CTTGGCTCTCTGTCTGTCCAGTT (all purchased from Greiner Bio-One International GmbH, Kremusmunster, Australia). SYBR Premix Ex Taq was purchased from TaKaRa (Tokyo, Japan).

2.7. Statistical analysis

All of the experiments were repeated at least three times. All data are presented as the mean ± SD. Differences between data were determined by Student's t-test with STATCEL3 (OMS Inc., Tokorozawa, Japan).

3. Results

3.1. p62-deficient MEFs showed resistance to UVB-induced apoptosis

To test whether p62 is involved in UVB-induced apoptosis, MEFs derived from $p62^{-/-}$ and $p62^{+/+}$ mice were irradiated with UVB at 300 and 600 mJ/cm^2, and the apoptosis ratio was determined by FACS with Annexin V/PI double immunostaining. Figures 2A and B show representative scatterplots of $p62^{-/-}$ and $p62^{+/+}$ MEFs; the upper- and lower-right areas in the scatterplot indicate late and early apoptosis, respectively. Compared to $p62^{+/+}$ MEFs, the $p62^{-/-}$ MEFs had significantly fewer cells plotted in the apoptosis area. Figure 2C shows that the apoptosis ratio (as defined in Materials and Methods) was significantly lower in $p62^{-/-}$ MEFs than in $p62^{+/+}$ MEFs; thus, UVB-induced apoptosis was reduced in the $p62^{-/-}$ MEFs. To confirm that this reduction in apoptosis depended on the p62 deficiency, we knocked down p62 in HaCaT cells (a human keratinocyte cell line) by transfection with p62-specific siRNA and subjected the cells to UVB radiation. The apoptosis ratio was significantly lower in the p62-knockdown than in the control HaCaT cells, indicating that the p62-knockdown cells were more resistant to UVB-induced apoptosis (Fig 2D).

3.2. UVB induced the expression of Bcl-2 family proteins in p62-deficient MEFs

The upregulation of Bcl-2 or Bcl-xL is essential in apoptosis [4]. Thus, we exposed $p62^{-/-}$ and $p62^{+/+}$ MEFs to UVB radiation and determined the Bcl-2, Bcl-xL, and Bax levels by western blot. Although the expression of all of these molecules decreased after

300 mJ/cm^2 UVB irradiation (Fig. 3A-D), the Bcl-2 remained significantly higher in p62$^{-/-}$ than in p62$^{+/+}$ MEFs ($P < 0.001$), while the Bax was significantly lower ($P < 0.001$).

3.3. Gene expression of factors associated with UVB irradiation in p62-deficient MEFs

Since the Bcl-2 and Bax expressions differed significantly between p62$^{+/+}$ and p62$^{-/-}$ MEFs prior to UVB irradiation, we used real-time PCR in the steady state to examine the mRNA levels of factors associated with UV-induced apoptotic signaling [4, 21-24]. In this experiment, we examined ATM, PUMA, NOXA, and survivin in addition to Bcl-2, Bcl-xL, and Bax (Fig 4A-G). We found that the Bcl-2 and Bcl-xL mRNA levels were significantly increased in p62$^{-/-}$ MEFs, while those of Bax and NOXA were decreased (Fig. 4A, B, C, E).

3.4. Src and Stat3 phosphorylation in p62-deficient MEFs and in apoptosis

It was previously found that the nuclear translocation of Stat3 is increased in p62$^{-/-}$ mice compared with p62$^{+/+}$ control mice [15]. The upregulation of both Bcl-2 and Bcl-xL increases a cell's resistance to apoptosis [4]. Bcl-2 and Bcl-xL are regulated by Stat3, which acts downstream of growth factors and oncogenic kinases [25]. In addition, Src signaling can activate downstream signaling pathways that control survival, and Stat3 acts downstream of Src [26]. Thus, weexamined Src and Stat3 phosphorylation by western blot to analyze apoptotic signals.

Src and its downstream target Stat3 were phosphorylated in the steady state in p62$^{-/-}$ MEFs, but were rarely phosphorylated in p62$^{+/+}$ MEFs (Fig. 5A). Figures 5B and 5C show

the ratio of phosphorylated protein to whole protein. The proportion of phosphorylated Src was 8.1 ± 4.1% in $p62^{+/+}$ MEFs, and 25.8 ± 3.5% in $p62^{-/-}$ MEFs. The proportion of phosphorylated Stat3 was 1.5 ± 0.2% in $p62^{+/+}$ MEFs, and 20.2 ± 7.6% in $p62^{-/-}$ MEFs. Thus, the proportion of phosphorylated Src and Stat3 was significantly higher in $p62^{-/-}$ MEFs than in $p62^{+/+}$ MEFs.

Next, we used PP2, a inhibitor for Src-family kinases, to examine whether inhibiting the Src phosphorylation could regulate the Stat3 phosphorylation. Increasing the concentration of PP2 from 0 to 20 μM, by degrees, gradually reduced the Stat3 phosphorylation in $p62^{-/-}$ MEFs (Fig. 6A). To test whether the resistance to apoptosis in $p62^{-/-}$ MEFs was due to Src phosphorylation, we tested the effect of UVB radiation on PP2-treated or untreated cells. Without PP2 treatment, the apoptosis ratio after 300 and 600 mJ/cm^2 irradiation was 33.9 ± 3.2% respectively, and 45.4 ± 5.4% in $p62^{+/+}$ MEFs, and 15.6 ± 0.7% and 25.3 ± 0.7% in $p62^{-/-}$ MEFs. With PP2 treatment, the apoptosis ratio after 300 and 600 mJ/cm^2 irradiation was 42.8 ± 5.0%, and 64.8 ± 4.3% respectively in $p62^{+/+}$ MEFs, and 40.2 ± 8.6% and 57.9 ± 13.1% in $p62^{-/-}$ MEFs. Thus, the apoptosis ratio in PP2-treated $p62^{-/-}$ MEFs after UVB irradiation was recovered to a level similar to that of $p62^{+/+}$ MEFs (Fig. 6B). These results suggested that Src phosphorylation regulated the Stat3 phosphorylation and reduced the UVB-induced apoptosis.

4. Discussion

In this study, we showed that $p62^{-/-}$ cells were significantly more resistant than $p62^{+/+}$ cells to UVB-induced apoptosis. Although $p62^{-/-}$ MEFs lack p62 due to a defective gene, and are therefore suitable for assessing the role of the p62 protein, we considered the possibility that $p62^{-/-}$ MEFs were changed by passaging in the absence of the gene, and thus that the difference was a secondary effect caused by changes in the nature of the cells themselves. To rule out this possibility, we investigated the UVB-induced apoptosis in siRNA knockdown cells, and found that p62 knockdown HaCaT cells generated by the transient suppression by siRNA were also significantly more resistant to apoptosis than the control HaCaT cells. Thus, p62 deficiency increased resistance to apoptosis regardless of whether the deficiency was generated by gene knockout or siRNA knockdown, supporting the involvement of p62 in UVB-induced apoptosis signaling.

Currently, p53 is thought to mediate mitochondria-dependent apoptosis by interacting directly with mitochondria and members of the Bcl-2 family of apoptosis-regulating proteins [21]. When UV exposure damages DNA, p53 upregulates the pro-apoptotic proteins Bax, Bak, PUMA, and Noxa in concert with the trans-repression of the anti-apoptotic proteins Bcl-2 and Bcl-xL [27]. On the other hand, the PIKK proteins, including DNA-dependent kinase, ATM (Ataxia Telangiectasia Mutated), and ATR (ATM and Rad3 Related), are involved in early signals provided by DNA-damage processing responses [24].

In the present study, we found significantly higher Bcl-2 expression and lower Bax expression in $p62^{-/-}$ MEFs compared to $p62^{+/+}$ MEFs, both before and after UVB

irradiation. In the steady state, the Bcl-2 and Bcl-xL mRNAs were elevated in non-irradiated $p62^{-/-}$ cells. Bcl-2 and Bcl-xL are localized to the mitochondrial membrane and maintain its permeability [28]. Upon UVB-induced or other cell damage, Bcl-2 and Bcl-xL are suppressed, and Bax and Bak bind to the mitochondrial membrane and increase its permeability, causing mitochondrial cytochrome C (CytC) to leak into the cytoplasm where it triggers caspase activation [28]. Consequently, apoptosis is reduced by decreasing the Bax expression, and by increasing the expression of Bcl-2 and Bcl-xL. Here, we found that $p62^{-/-}$ MEFs resisted UVB-induced apoptosis because of alterations in the steady-state levels of Bcl-2-family proteins. Our results are also supported by our previous finding that $p62^{-/-}$ MEFs are highly proliferative [14].

We previously observed that leptin treatment changes the Stat3 dynamics in $p62^{-/-}$ MEFs [15]. In the present study, we examined the Stat3 phosphorylation in $p62^{-/-}$ MEFs. Stat3 increases the expression of apoptosis inhibitors such as Bcl-2 or Bcl-xL and simultaneously stimulates the expression of cyclin and other factors that enhance the cell cycle, thereby preventing apoptosis during cell proliferation [29]. Thus, Stat3's phosphorylation is inhibited with some cause, decreasing the expression of its target genes, such as Bcl-2 [30]. On the other hand, the Src family of protein kinases and JAK can regulate Stat3 phosphorylation in response to growth factor-initiated signals [26]. In our preliminary study, we found that inhibiting JAK did not affect Stat3's phosphorylation level in $p62^{-/-}$ MEFs in the steady state (data not shown), so we focused on Src signaling. Src is located downstream of growth factor signals such as PDGF and EGF [31]. Activation of EGF and PDGF receptors results in the phosphorylation on tyrosine residues of Src via Ras, leading to the phosphorylation of growth factor signals such as

the transcription factor Stat3. As expected, we found here that Src and Stat3 were phosphorylated at significantly higher levels in $p62^{-/-}$ MEFs than in $p62^{+/+}$ MEFs at steady state, and the Src inhibitor PP2 eliminated the Stat3 phosphorylation and recovered apoptosis. From these results, we can hypothesize that one of the points of p62 action is upstream of Src in the UVB-induced apoptosis-signaling pathway, though recent report shows PP2 has off-target effects[32] and there may be another target.

In this study, we focused on UVB-induced apoptosis and analyzed the role of p62 in apoptosis, especially in intrinsic apoptotic signaling. p62 is a multifunctional adaptor protein that is associated with NFκB, Nrf2-keap1, and mTOR signaling [33]. In particular, p62 associates with the mTOR complex via raptor to orchestrate autophagy [34]. The AKT/mTOR pathway counteracts p53 and impedes UV-induced apoptosis [27]. Furthermore, UVRAG (UV radiation resistance-associated gene) activates Beclin-1 (Bcl-2 interacting protein 1; ATG6), which orchestrates the initial steps in autophagosome formation [27, 35]. There may be additional pathways that modulate UV-induced apoptosis that relate to autophagic factors. Further study will be necessary to elucidate other possible mechanisms that modulate signals in UVB-induced apoptosis.

In conclusion, our results indicate that p62 deficiency modified the apoptotic signaling in $p62^{-/-}$ MEFs in a manner that reduced UVB-induced apoptosis. It is likely that one of the causative factors is involved in phosphorylating Src or its upstream receptor, tyrosine kinase. The p62 deficiency increased the Src phosphorylation and Stat3 phosphorylation, leading to increased Bcl-2 and Bcl-xL expression. These changes modified the intrinsic UVB-induced apoptosis signal, resulting in a resistance to apoptosis.

Fig.1

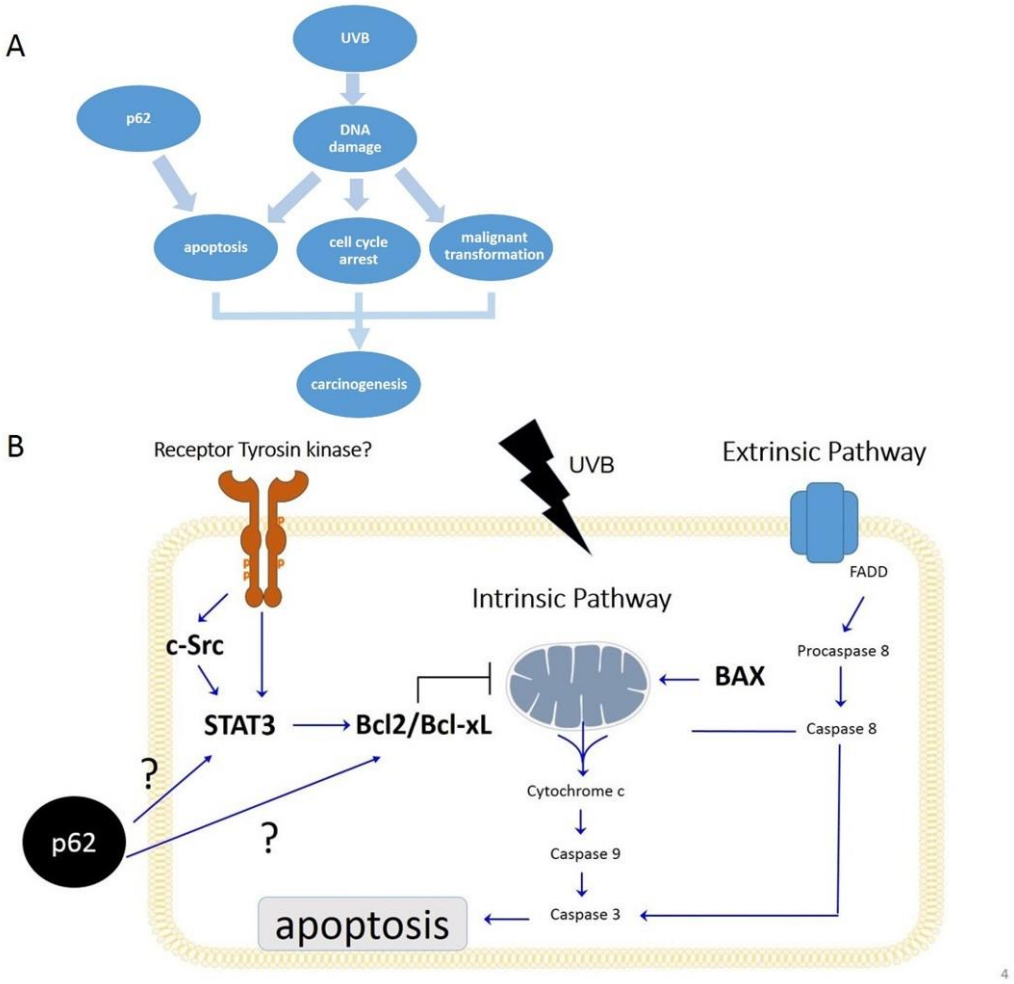
A
UVB
p62
DNA damage
apoptosis
cell cycle arrest
malignant transformation
carcinogenesis
B
Receptor Tyrosin kinase?
UVB
Extrinsic Pathway
FADD
Intrinsic Pathway
c-Src
Procaspase 8
BAX
STAT3
Bcl2/Bcl-xL
Caspase 8
?
Cytochrome c
p62
?
Caspase 9
Caspase 3
apoptosis

Fig.1. Scheme of this study

Panel A : One of the important risks of skin cancer is the ultraviolet radiation, particularly UVB radiation. When the epidermal cells get unrecoverable damages by UVB radiation, malignant transformation is avoided as the damage is eliminated by apoptosis. Therefore, suppression of the apoptosis machinery is thought to lower the threshold for the occurrence of a cancer. The overexpression of p62 has been found in various cancers such as lung carcinoma and hepatocellular carcinoma in recent years, so it is recognized to be involved in the cancer development

Panel B : We have therefore studied on p62-deficient mice to find whether p62 is likely to act on promoting tumor or suppressing it in the skin by investigating the movement of p62 in apoptosis after damaging the DNA with the ultraviolet radiation which is a major cause of skin cancer. If apoptosis is suppressed by p62 deficiency, the threshold of cancer occurrence will be lowered accordingly. For that reason, this time we have studied on factors related to endogenous apoptosis such as Bcl-2 family proteins and its upstream of STAT3 in order to investigate the relationship between endogenous apoptosis and p62.

Fig. 2

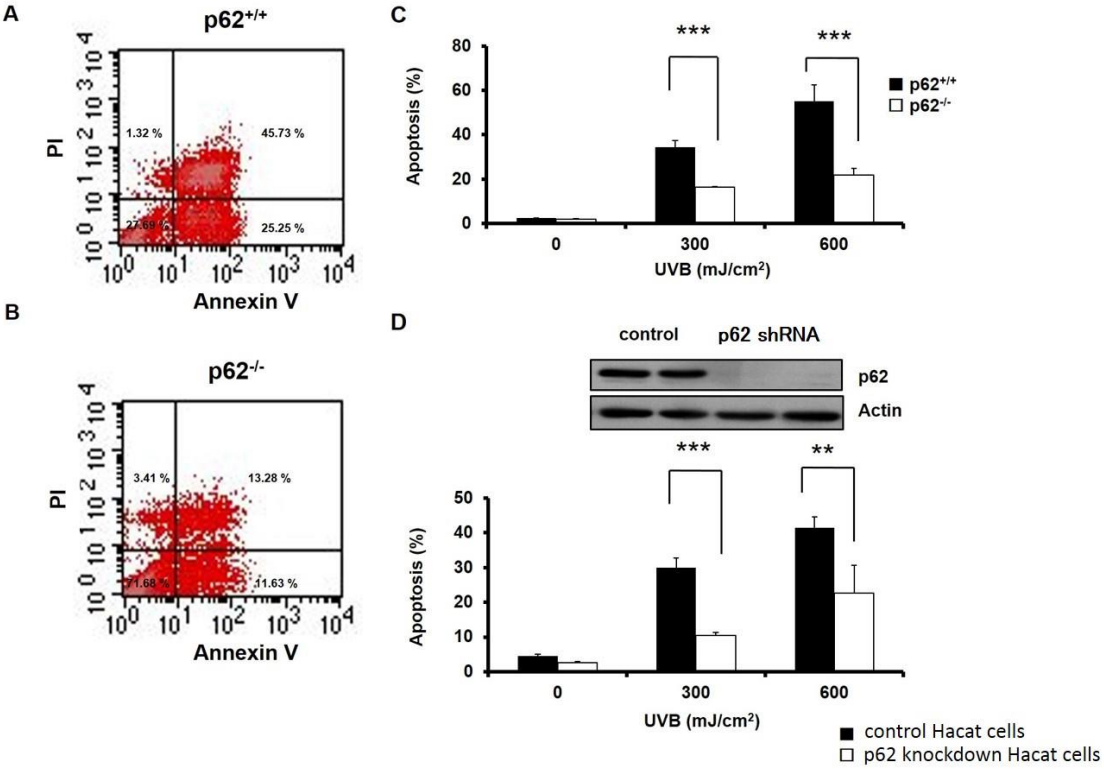
A
p62+/+
PI
Annexin V
1.32 %
45.73 %
27.69 %
25.25 %
B
p62-/-
3.41 %
13.28 %
71.68 %
11.63 %
C
Apoptosis (%)
UVB (mJ/cm2)
***
***
p62+/+
p62-/-
D
control
p62 shRNA
p62
Actin
**
control Hacat cells
p62 knockdown Hacat cells

Fig. 2. Apoptosis ratio of p62-deficient cells, analyzed by flow cytometry.

Panels A and B: representative scatterplots of $p62^{+/+}$ and $p62^{-/-}$ MEFs, respectively. The upper-right area indicates cells in late apoptosis and the lower-right area indicates early apoptosis; $p62^{+/+}$ MEFs had more cells in the apoptosis area than did $p62^{-/-}$ MEFs.

Panel C: Apoptosis ratio of $p62^{+/+}$ (black bars) and $p62^{-/-}$ MEFs (white bars) with and without UVB irradiation, determined by flow cytometry analysis (FACS). The percentage of apoptotic cells was significantly lower in $p62^{-/-}$ MEFs than in $p62^{+/+}$ MEFs after UVB exposure at 300 and 600 mJ/cm^2.

The apoptosis ratio of $p62^{+/+}$ MEFs at 0, 300, and 600 mJ/cm^2 was 2.41 ± 0.12%, 34.47 ± 2.86%, and 55.14 ± 7.40%, respectively, and that of $p62^{-/-}$ MEFs was 1.97 ± 0.31%, 16.35 ± 0.46%, and 21.96 ± 2.84%, respectively.

Panel D: Apoptosis ratio of p62-knockdown HaCaT cells with and without UVB irradiation, determined by FACS. Upper panel, immunoblot for p62 demonstrating that p62 was absent in the p62-knockdown cells.

Compared to control cells (black bars), apoptosis was significantly reduced in cells treated with p62 siRNA (knockdown cells, white bars); cells were irradiated at 300 and 600 mJ/ cm^2. The apoptosis ratio of control cells at 0, 300, and 600 mJ/cm^2 was 4.58 ± 0.48%, 29.87 ± 2.89%, and 41.41 ± 3.20%, respectively; that of p62-knockdown cells was 2.60 ± 0.31%, 10.37 ± 1.02%, and 22.70 ± 7.87%, respectively. Values are shown as mean ± standard deviation. **P<0.01, ***P<0.001.

Fig.3

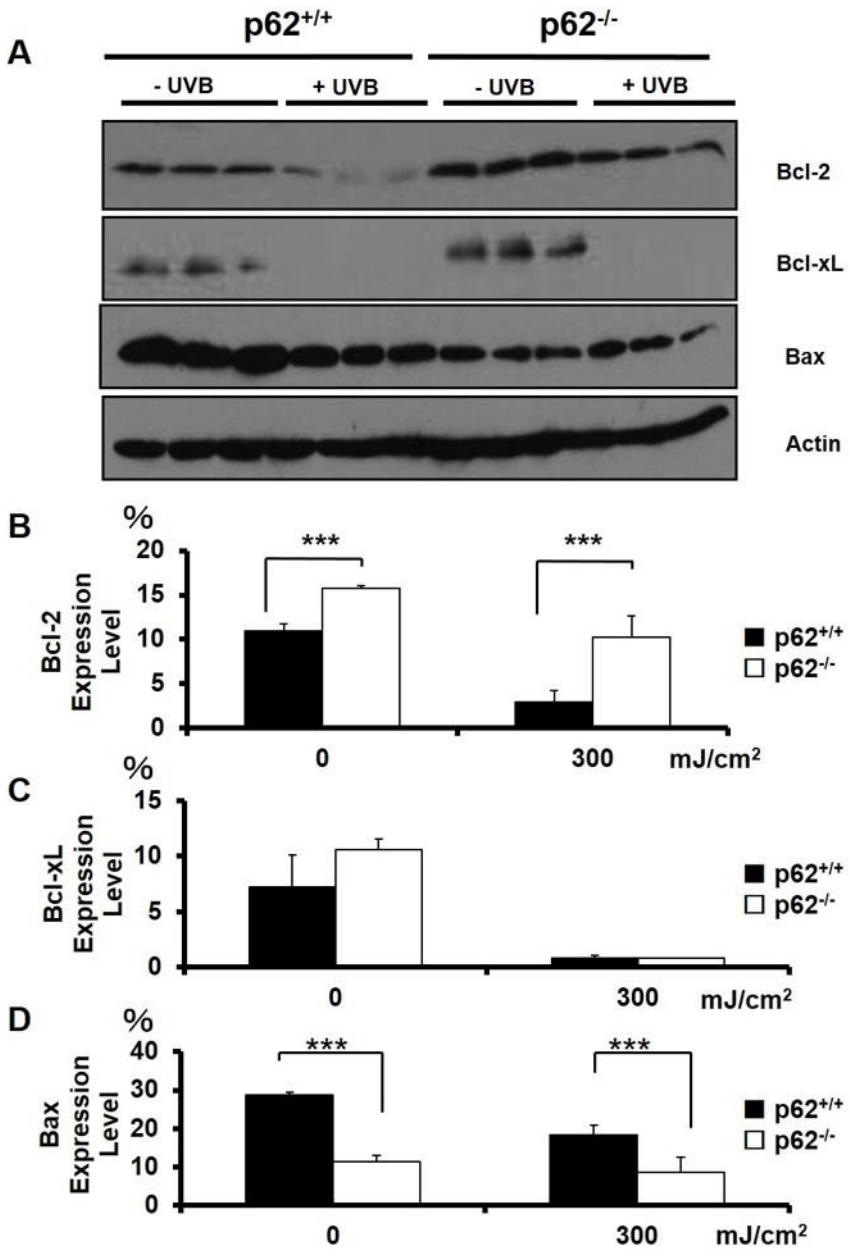
A
p62+/+
p62-/-
- UVB
+ UVB
- UVB
+ UVB
Bcl-2
Bcl-xL
Bax
Actin
B
%
Bcl-2 Expression Level
20
15
10
5
0
***
***
p62+/+
p62-/-
0
300
mJ/cm2
C
%
Bcl-xL Expression Level
15
10
5
0
p62+/+
p62-/-
0
300
mJ/cm2
D
%
Bax Expression Level
40
30
20
10
0
***
***
p62+/+
p62-/-
0
300
mJ/cm2

Fig. 3. Immunoblotting analysis of Bcl-2, Bcl-xL, and Bax.

Panel A: Immunoblotting for Bcl-2, Bcl-xL, and Bax in $p62^{-/-}$ and $p62^{+/+}$ MEFs with or without UVB irradiation (300 mJ/cm$^{2)}$.

Panel B: Bcl-2 expression, quantified by immunoblotting, was significantly higher in $p62^{-/-}$ MEFs (white bars) than in $p62^{+/+}$ MEFs (black bars). Bcl-2 expression levels after 0 and 300 mJ/cm^2 irradiation were 10.99 ± 0.74% and 2.90 ± 1.33% for $p62^{+/+}$ MEFs, and 15.75 ± 0.34% and 10.23 ± 2.38% for $p62^{-/-}$ MEFs.

Panel C: Bcl-xL expression, quantified by immunoblotting, did not differ significantly between the $p62^{+/+}$ and $p62^{-/-}$ MEFs. Bcl-xL levels after irradiation with 0 and 300 mJ/cm^2 were 7.19 ± 2.92% and 0.86 ± 0.18% for $p62^{+/+}$ MEFs, and 10.56 ± 0.98% and 0.80 ± 0.05% for $p62^{-/-}$ MEFs.

Panel D: Bax expression, quantified by immunoblotting, was significantly lower in $p62^{-/-}$ MEFs than in $p62^{+/+}$ MEFs. Bax levels after irradiation with 0 and 300 mJ/cm^2 were 28.85 ± 0.67% and 18.42 ± 2.54% for $p62^{+/+}$ MEFs, and 11.31 ± 1.73% and 8.69 ± 3.87% for $p62^{-/-}$ MEFs. Each value was determined as a percentage of sample density relative to the actin control density. Values are shown as mean ± standard deviation. **P<0.01, ***P<0.001.

Fig. 4

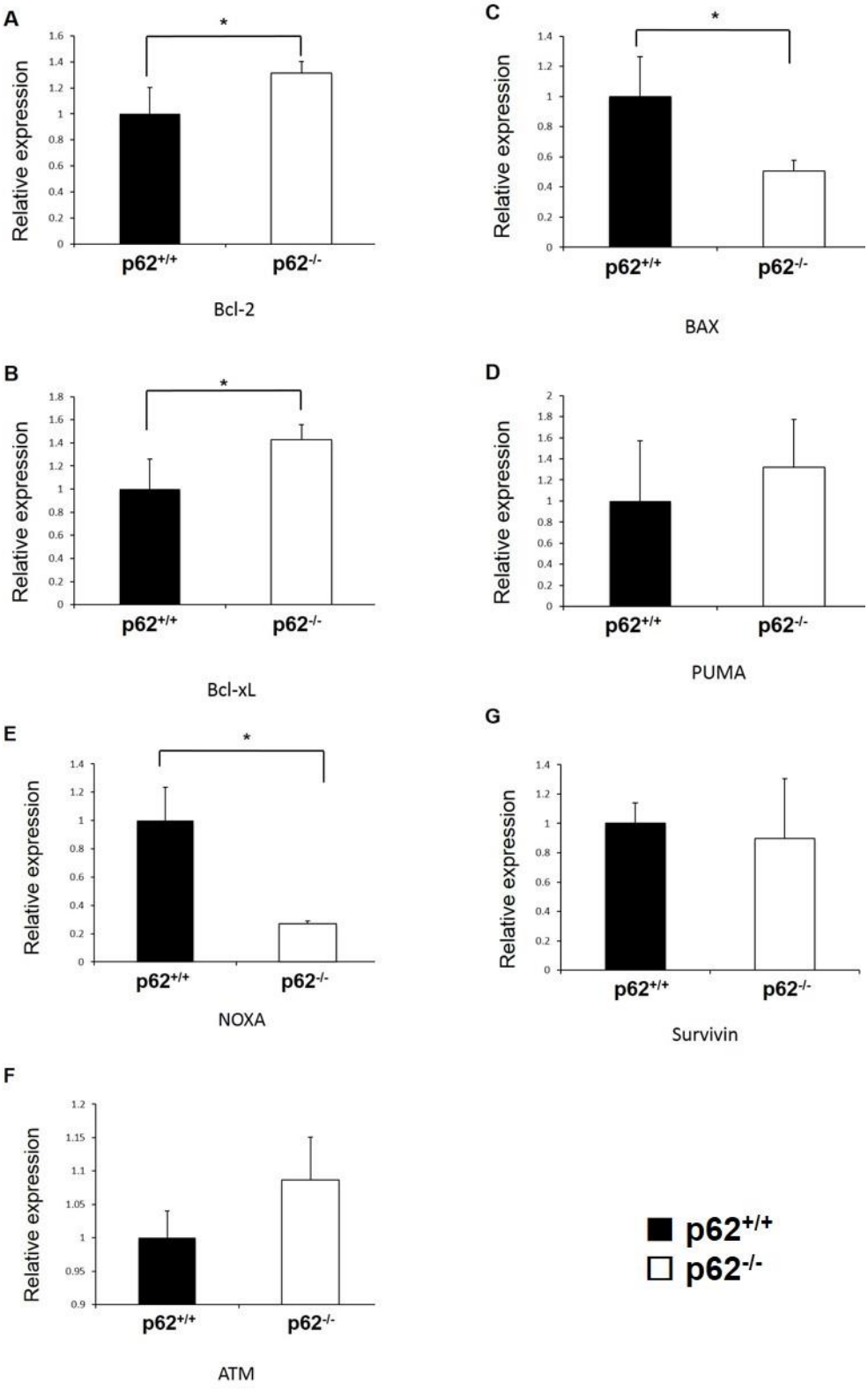
A
Relative expression
*
p62+/+
p62-/-
Bcl-2
C
Relative expression
*
p62+/+
p62-/-
BAX
B
Relative expression
*
p62+/+
p62-/-
Bcl-xL
D
Relative expression
p62+/+
p62-/-
PUMA
E
Relative expression
*
p62+/+
p62-/-
NOXA
G
Relative expression
p62+/+
p62-/-
Survivin
F
Relative expression
p62+/+
p62-/-
ATM
p62+/+
p62-/-

Fig. 4. Quantitative PCR analysis of the mRNAs for factors associated with UV-induced apoptosis in $p62^{+/+}$ and $p62^{-/-}$ MEFs.

The mRNA expression levels in $p62^{-/-}$ MEFs (white bars) were determined relative to those in $p62^{+/+}$ MEFs (defined as 1.00; black bars).

Panel A: Bcl-2 mRNA expression in $p62^{+/+}$ and $p62^{-/-}$ MEFs, with values of 1.00 ± 0.20 and 1.31 ± 0.09, respectively. Bcl-2 mRNA expression was significantly higher in $p62^{-/-}$ MEFs than in $p62^{+/+}$ MEFs.

Panel B: Bcl-xL mRNA expression in $p62^{+/+}$ and $p62^{-/-}$ MEFs, with values of 1.00 ± 0.26 and 1.43 ± 0.13, respectively. Bcl-xL mRNA expression was significantly higher in $p62^{-/-}$ MEFs than in $p62^{+/+}$ MEFs.

Panel C: Bax mRNA expression in $p62^{+/+}$ and $p62^{-/-}$ MEFs, with values of 1.00 ± 0.26 and 0.50 ± 0.07, respectively. Bax mRNA expression was significantly lower in $p62^{-/-}$ MEFs than in $p62^{+/+}$ MEFs.

Panel D: PUMA mRNA expression in $p62^{+/+}$ and $p62^{-/-}$ MEFs, with values of 1.00 ± 0.57 and 1.31 ± 0.46, respectively.

Panel E: NOXA mRNA expression in $p62^{+/+}$ and $p62^{-/-}$ MEFs, with values of 1.00 ± 0.24 and 0.27 ± 0.02, respectively. NOXA mRNA expression was significantly lower in $p62^{-/-}$ MEFs than in $p62^{+/+}$ MEFs.

Panel F: ATM mRNA expression in $p62^{+/+}$ and $p62^{-/-}$ MEFs, with values of 1.00 ± 0.04 and 1.08 ± 0.06, respectively.

Panel G: Survivin mRNA expression in $p62^{+/+}$ and $p62^{-/-}$ MEFs, with values of 1.00 ± 0.13 and 0.89 ± 0.41, respectively.

Values are shown as mean ± standard deviation. *P<0.05.

Fig. 5

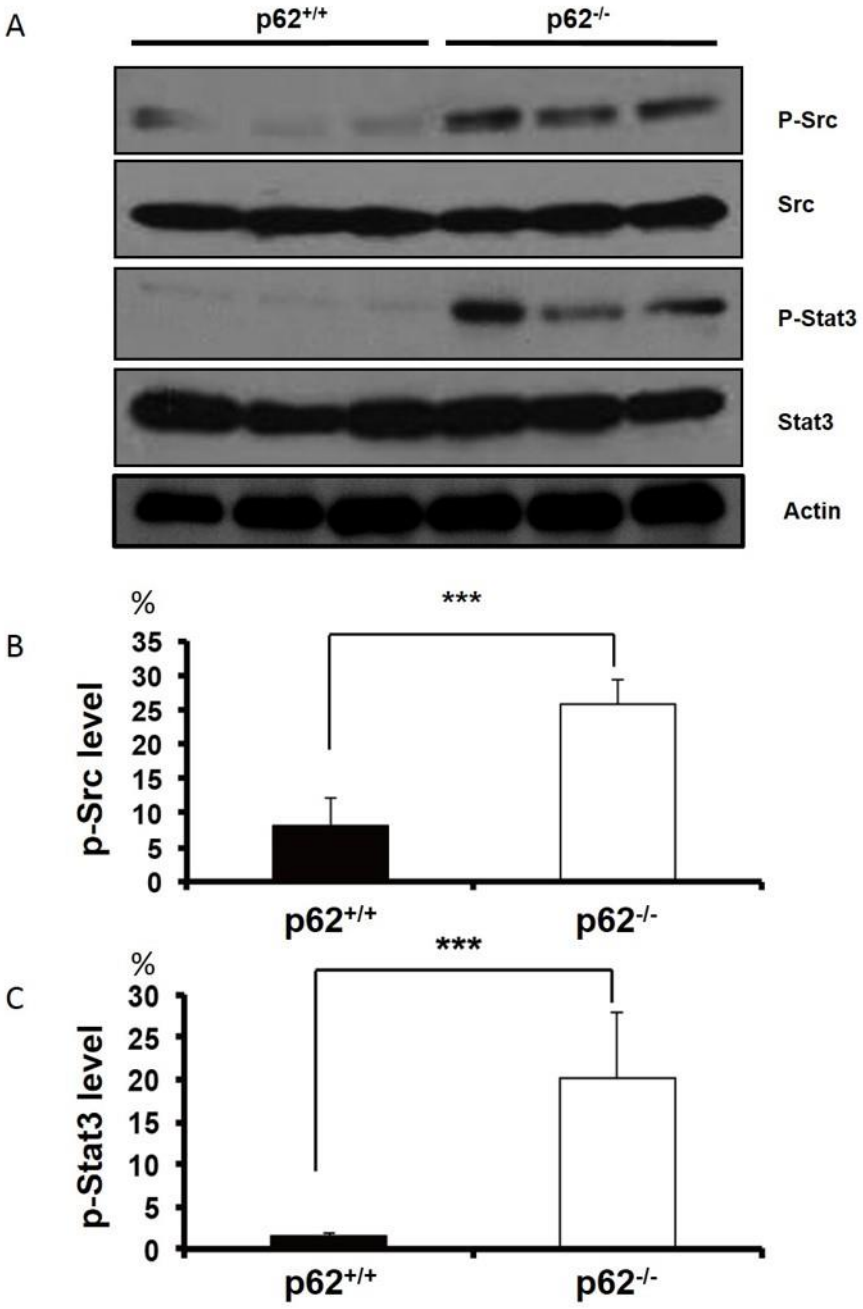
A
p62+/+
p62-/-
P-Src
Src
P-Stat3
Stat3
Actin
B
%
***
p-Src level
35
30
25
20
15
10
5
0
p62+/+
p62-/-
C
%
***
p-Stat3 level
30
25
20
15
10
5
0
p62+/+
p62-/-

Fig. 5. Src and Stat3 phosphorylation in $p62^{-/-}$ and $p62^{+/+}$ MEFs.

Panel A: Immunoblots of phosphorylated Src and Stat3 showing that the phosphorylation of Src and Stat3 in the steady state was increased in $p62^{-/-}$ MEFs compared with $p62^{+/+}$ MEFs.

Panel B: The proportion of phosphorylated Src (p-Src) was significantly higher in $p62^{-/-}$ MEFs than in $p62^{+/+}$ MEFs, as determined by immunoblots.

Panel C: The proportion of phosphorylated Stat3 (p-Stat3) was significantly higher in $p62^{-/-}$ MEFs than in $p62^{+/+}$ MEFs, as determined by immunoblots.

Values are shown as mean ± standard deviation. ***P<0.001.

Fig. 6

A

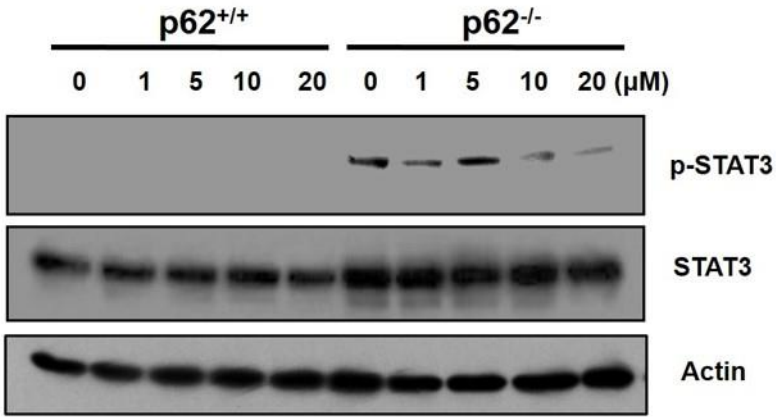
p62+/+
p62-/-
0 1 5 10 20 0 1 5 10 20 (μM)
p-STAT3
STAT3
Actin

B

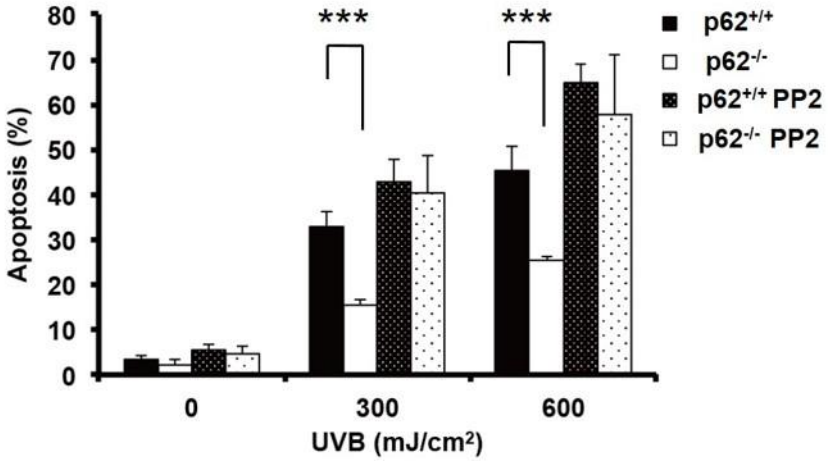
Apoptosis (%)
80
70
60
50
40
30
20
10
0
***
***
0
300
600
UVB (mJ/cm2)
p62+/+
p62-/-
p62+/+ PP2
p62-/- PP2

Fig. 6. Decreased Stat3 phosphorylation and increased apoptosis in UVB-irradiated $p62^{-/-}$ MEFs treated with a Src inhibitor.

Panel A: Stat3 phosphorylation was inhibited by PP2, a inhibitor for Src-family kinases. Immunoblots for Stat3 and phosphorylated Stat3 in $p62^{-/-}$ and $p62^{+/+}$ MEFs that were UVB-irradiated at 300 mJ/cm^2 and treated with PP2 at the indicated dose. In $p62^{-/-}$ MEFs, Stat3 was phosphorylated before UVB irradiation, and as the PP2 dose increased, the Stat3 phosphorylation decreased.

Panel B: The apoptosis ratio in PP2-treated or untreated $p62^{-/-}$ and $p62^{+/+}$ MEFs after UVB irradiation, analyzed by flow cytometry. The apoptosis ratio of $p62^{-/-}$ MEFs after UVB irradiation was significantly lower than that of $p62^{+/+}$ MEFs at 300 and 600 mJ/cm^2. However, after adding 20 μM PP2, the difference in apoptosis ratio between $p62^{-/-}$ and $p62^{+/+}$ MEFs was eliminated.

Values are shown as mean ± standard deviation. ***P<0.001.

References

[1] Ultraviolet damage, DNA repair and vitamin D in nonmelanoma skin cancer and in malignant melanoma: an update.
[2] Pustisek N, Situm M: UV-radiation, apoptosis and skin. Coll Antropol 35 Suppl 2: 339-341, 2011.
[3] Lee CH, Wu SB, Hong CH, Yu HS, Wei YH: Molecular Mechanisms of UV-Induced Apoptosis and Its Effects on Skin Residential Cells: The Implication in UV-Based Phototherapy. Int J Mol Sci 14: 6414-6435, 2013.
[3] Nys K, Agostinis P: Bcl-2 family members: essential players in skin cancer. Cancer Lett 320: 1-13, 2012.
[5] Moscat J, Diaz-Meco MT: p62: a versatile multitasker takes on cancer. Trends Biochem Sci 37: 230-236, 2012.
[6] Ishii T, Yanagawa T, Kawane T, Yuki K, Seita J, Yoshida H, Bannai S: Murine peritoneal macrophages induce a novel 60-kDa protein with structural similarity to a tyrosine kinase p56lck-associated protein in response to oxidative stress. Biochem Biophys Res Commun 226: 456-460., 1996.
[7] Komatsu M, Waguri S, Koike M, Sou YS, Ueno T, Hara T, Mizushima N, Iwata J, Ezaki J, Murata S, Hamazaki J, Nishito Y, Iemura S, Natsume T, Yanagawa T, Uwayama J, Warabi E, Yoshida H, Ishii T, Kobayashi A, Yamamoto M, Yue Z, Uchiyama Y, Kominami E, Tanaka K: Homeostatic Levels of p62 Control Cytoplasmic Inclusion Body Formation in Autophagy-Deficient Mice. Cell 131: 1149-1163, 2007.
[8] Moscat J, Diaz-Meco MT: p62 at the crossroads of autophagy, apoptosis, and cancer. Cell 137: 1001-1004, 2009.
[9] Mathew R, Karp CM, Beaudoin B, Vuong N, Chen G, Chen HY, Bray K, Reddy A, Bhanot G, Gelinas C, Dipaola RS, Karantza-Wadsworth V, White E: Autophagy suppresses tumorigenesis through elimination of p62. Cell 137: 1062-1075, 2009.
[10] Maiuri MC, Zalckvar E, Kimchi A, Kroemer G: Self-eating and self-killing: crosstalk between autophagy and apoptosis. Nat Rev Mol Cell Biol 8: 741-752, 2007.
[11] Duran A, Linares JF, Galvez AS, Wikenheiser K, Flores JM, Diaz-Meco MT, Moscat J.: The signaling adaptor p62 is an important NF-kappaB mediator in tumorigenesis.Cancer Cell 13.343-354,2008
[12] Yoshihara N, Takagi A, Ueno T, Ikeda S: Inverse correlation between microtubule-associated protein 1A/1B-light chain 3 and p62/sequestosome-1 expression in the progression of cutaneous squamous cell carcinoma. Journal of Dermatology 41:311-315,2014
[13] Ellis RA, Horswell S, Ness T, Lumsdon J, Tooze SA, Kirkham N, Armstrong JL, Lovat PE: Prognostic impact of p62 expression in cutaneous malignant melanoma. J Invest Dermatol 134(5) : 1476–1478,2014
[14] Sugimoto R, Warabi E, Katayanagi S, Sakai S, Uwayama J, Yanagawa T, Watanabe A, Harada H, Kitamura K, Noguchi N, Yoshida H, Siow RC, Mann GE, Ishii T: Enhanced neointimal hyperplasia and carotid artery remodelling in sequestosome 1 deficient mice. J Cell Mol Med 14: 1546-1554, 2010.
[15] Harada H, Warabi E, Matsuki T, Yanagawa T, Okada K, Uwayama J, Ikeda A, Nakaso K, Kirii K, Noguchi N, Bukawa H, Siow RC, Mann GE, Shoda J, Ishii T, Sakurai T: Deficiency of p62/Sequestosome 1 causes hyperphagia due to leptin resistance in the

brain. J Neurosci 33: 14767-14777, 2013.
[16] Ito T, Kimura S, Seto K, Warabi E, Kawachi Y, Shoda J, Tabuchi K, Yamagata K, Hasegawa S, Bukawa H, Ishii T, Yanagawa T: Peroxiredoxin I plays a protective role against UVA irradiation through reduction of oxidative stress. J Dermatol Sci 74: 9-17, 2014.
[17] Hirota A, Kawachi Y, Yamamoto M, Koga T, Hamada K, Otsuka F: Acceleration of UVB-induced photoageing in nrf2 gene-deficient mice. Exp Dermatol 20: 664-668, 2011.
[18] Hirota A, Kawachi Y, Itoh K, Nakamura Y, Xu X, Banno T, Takahashi T, Yamamoto M, Otsuka F: Ultraviolet A irradiation induces NF-E2-related factor 2 activation in dermal fibroblasts: protective role in UVA-induced apoptosis. J Invest Dermatol 124: 825-832, 2005.
[19] Kimura S, Warabi E, Yanagawa T, Ma D, Itoh K, Ishii Y, Kawachi Y, Ishii T: Essential role of Nrf2 in keratinocyte protection from UVA by quercetin. Biochem Biophys Res Commun 387: 109-114, 2009.
[20] Warabi E, Takabe W, Minami T, Inoue K, Itoh K, Yamamoto M, Ishii T, Kodama T, Noguchi N: Shear stress stabilizes NF-E2-related factor 2 and induces antioxidant genes in endothelial cells: role of reactive oxygen/nitrogen species. Free Radic Biol Med 42: 260-269, 2007.
[21] Assefa Z, Van Laethem A, Garmyn M, Agostinis P: Ultraviolet radiation-induced apoptosis in keratinocytes: on the role of cytosolic factors. Biochim Biophys Acta 1755: 90-106, 2005.
[22] Dallaglio K, Marconi A, Pincelli C: Survivin: a dual player in healthy and diseased skin. J Invest Dermatol 132: 18-27, 2012.
[23] Naik E, Michalak EM, Villunger A, Adams JM, Strasser A: Ultraviolet radiation triggers apoptosis of fibroblasts and skin keratinocytes mainly via the BH3-only protein Noxa. J Cell Biol 176: 415-424, 2007.
[24] Batista LF, Kaina B, Meneghini R, Menck CF: How DNA lesions are turned into powerful killing structures: insights from UV-induced apoptosis. Mutat Res 681: 197-208, 2009.
[25] Aggarwal BB, Sethi G, Ahn KS, Sandur SK, Pandey MK, Kunnumakkara AB, Sung B, Ichikawa H: Targeting signal-transducer-and-activator-of-transcription-3 for prevention and therapy of cancer: modern target but ancient solution. Ann N Y Acad Sci 1091: 151-169, 2006.
[26] Haura EB: SRC and STAT pathways. J Thorac Oncol 1: 403-405, 2006.
[27] Strozyk E, Kulms D: The role of AKT/mTOR pathway in stress response to UV-irradiation: implication in skin carcinogenesis by regulation of apoptosis, autophagy and senescence. Int J Mol Sci 14: 15260-15285, 2013.
[28] Ledgerwood EC, Morison IM: Targeting the apoptosome for cancer therapy. Clin Cancer Res 15: 420-424, 2009.
[29] Kim DJ, Angel JM, Sano S, DiGiovanni J: Constitutive activation and targeted disruption of signal transducer and activator of transcription 3 (Stat3) in mouse epidermis reveal its critical role in UVB-induced skin carcinogenesis. Oncogene 28: 950-960, 2009.
[30] Bito T, Sumita N, Masaki T, Shirakawa T, Ueda M, Yoshiki R, Tokura Y, Nishigori C: Ultraviolet light induces Stat3 activation in human keratinocytes and fibroblasts through reactive oxygen species and DNA damage. Exp Dermatol 19: 654-660, 2010.
31] Belsches AP, Haskell MD, Parsons SJ: Role of c-Src tyrosine kinase in EGF-induced

mitogenesis. Front Biosci 2: d501-518, 1997.
[32] Frauenstein K, Tigges J, Soshilov AA, Kado S, Raab N, Fritsche E, Haendeler J, Denison MS, Vogel CF,Haarmann-Stemmann T: Activation of the aryl hydrocarbon receptor by the widely used Src family kinase inhibitor 4-amino-5-(4-chlorophenyl)-7-(dimethylethyl)pyrazolo[3,4-d]pyrimidine (PP2). Arch Toxicol 89: 1329-1336, 2015.
[33] Puissant A, Fenouille N, Auberger P: When autophagy meets cancer through p62/SQSTM1. Am J Cancer Res 2: 397-413, 2012.
[34] Duran A, Amanchy R, Linares JF, Joshi J, Abu-Baker S, Porollo A, Hansen M, Moscat J,Diaz-Meco MT: p62 is a key regulator of nutrient sensing in the mTORC1 pathway. Mol Cell 44: 134-146, 2011.
[35] Liang C, Feng P, Ku B, Dotan I, Canaani D, Oh BH, Jung JU: Autophagic and tumour suppressor activity of a novel Beclin1-binding protein UVRAG. Nat Cell Biol 8: 688-699, 2006.